Heliyon 10 (2024) e34679

Contents lists available at ScienceDirect

Heliyon

journal homepage: www.cell.com/heliyon

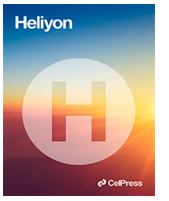

Research article

Experimental design of a film flow cleaning rig equipped with in-line process analytical technology (PAT) tool for real-time monitoring

Marina Steiner-Browne, Nicolas Abdel Karim Aramouni, Rabah Mouras *

Pharmaceutical Manufacturing Technology Centre (PMTC), Department of Chemical Sciences, Bernal Institute, University of Limerick, V94 T9XP, Limerick, Ireland

ARTICLE INFO

Keywords:
Cleaning
Rig
Monitoring
In-line
PAT
Spectroscopy

ABSTRACT

The main purpose of this research was to develop an experimental film flow cleaning rig that can be combined with Process analytical technology (PAT) tools to reduce cleaning time and costs. Here, we show that the use of in-line UV–Vis was successful for real-time monitoring of the cleaning process of olanzapine as a challenging residue to clean. The cleaning process was found to be affected by the properties of the olanzapine soil, and the study showed the competing effects of mechanical lift-off and dissolution action with methanol as a solvent. However, The method is limited by the cleaning mechanisms, with the dissolution being the only mechanism that can be accurately quantified using an in-line UV–Vis PAT tool. This experimental approach can be used to optimize cleaning process conditions and solvent choices at the bench scale before deployment. The material of which the cleaning rig was printed limited the solvent that could be used for this study, and future modifications will include a more chemical-resistant material.

1. Introduction

Cleanliness has to be guaranteed to prevent contamination of any pharmaceutical product [1]. There are no specific standards for verifying cleanliness criteria, with cleaning guidelines being determined by each company [2,3]. It is impossible to eliminate residuals left in the equipment after the cleaning totally, yet it is still possible to verify that the residuals left are below pre-determined acceptance limits [4,5]. Some of the historical acceptance limits that were adopted for cleaning validation are: dose, 10 ppm, and visually clean criteria [6]. For the first criterion, dose, a maximum of 0.1 % of the therapeutic dose can be carried out to the next product manufactured in the same equipment. For the second criterion, a maximum of 10 ppm of the product can appear in a different product. Finally, for the visually clean criterion, no residual should be visually observed on the equipment. The selection of the acceptance limit used will depend on the product being manufactured, and on the toxic and pharmacological potential of this product [7,8]. In recent years, Health-based exposure limits (HBELs) have become the standard criteria that are used to calculate cleaning limits, as mandated by the European Union's Good Manufacturing Practice (Annex 15) in 2015 [9]. This approach specifies the Permissible Daily Exposure (PDE) limit which sets a daily upper exposure limit with no adverse effects over a lifetime for the contaminant in question. This 'bottoms-up' approach constitutes a paradigm shift compared to other approaches that were based on LD_{50} or similar lethality measures.

* Corresponding author. Pharmaceutical Manufacturing Technology Centre University of Limerick – Limerick, Limerick, V94 T9PX, Ireland.
E-mail address: rabah.mouras@ul.ie (R. Mouras).

https://doi.org/10.1016/j.heliyon.2024.e34679
Received 8 February 2023; Received in revised form 8 July 2024; Accepted 15 July 2024
Available online 16 July 2024

The use of Process Analytical Technology (PAT) in cleaning verification is strongly encouraged [10]. Some of the analytical techniques that are used for cleaning verification are mid-IR [11,12], NIR [13], FT-IR [14], UV–Vis spectroscopy [15,16], fluorescence [17,18], total organic carbon (TOC) [17], LC-MS, LC-UV [16,19,20], and ultrasonic measurements [21]. UV–Vis spectroscopy generally has lower detection limits than other PAT techniques and is thus one of the most useful PAT tools in in-situ cleaning monitoring and verification. There are two main uses of PAT tools in cleaning: they allow for (i) the study of cleaning profiles, and (ii) the determination of cleaning endpoint. While the adoption of PAT and Quality by Design principles is still sluggish in the pharmaceutical industry [22,23], its use in process development can be very insightful. Notably, the study of cleaning profiles is useful to optimize cleaning procedures [24] before validation, in turn yielding more resource-efficient and more sustainable procedures. The removal of soils from process surfaces during cleaning-in-place (CIP) occurs by different mechanisms, such as [6] dissolution, shear off, and wash out. A typical CIP cycle consists of an initial gross clean [7] where the majority of the soil is mechanically removed from the surfaces by shearing and impact from the CIP jets. Subsequent cleaning cycles aim at the removal of a bound layer of soil, the majority of which is then removed by dissolution. Only dissolution can be properly quantified by UV–Vis. The main objective of this study was to design an experimental film flow rig that could be combined with an in-line UV–Vis PAT tool to study cleaning conditions in a CIP system. There is a need to improve cleaning, reducing downtime, cleaning time, and waste [25]. Here, we report the design and operation of a cleaning rig that replicates film flow and shear stresses typical of CIP applications on a bench scale. The rig can be used to optimize the CIP process parameters in terms of the T.A.C.T variables (time, action, chemicals, temperature) [26] before scaling up, thus saving time and resources. Typical bench-scale cleaning research is performed using simple coupon immersion tests or jet impingement tests on coupons [27,28], while several efforts are made to study cleaning procedures on the resource-intensive pilot scale [24,29]. This study focuses on combining CIP and PAT using bench scale cleaning tests to study cleaning profiles in the film flow configuration.

2. Materials and methods

2.1. Materials

The active pharmaceutical ingredient (API) selected for this study was Olanzapine, which was kindly provided by Eli Lilly & Co (Ireland) Ltd. Olanzapine was selected as a model as it was described as a hard-to-clean API, so it constitutes an ideal residue to mimic the worst-case scenario. Methanol was purchased from Fisher Scientific (CAS no. 67-56-1).

2.2. Design of the experimental rig

The purpose of the cleaning rig is to hold a 2" × 2″ coupon stained with API and replicate the falling film flow that would be generated by static clean-in-place (CIP) nozzles inside a process vessel. Typical flow rates in such applications are around 100 L min^{-1}. $m^{-1}_{diameter}$, this specifies the range of flow rates of interest in the rig at up to 1.8 L min^{-1} for a 2″ wide channel, by normalisation of the flow rate to the perimeter. The flow rate used in this study was 0.8 L min^{-1}, which corresponds to a moderate flow rate sufficient to reach fully developed flow conditions that cover the entire coupon width. This was chosen to give a conservative estimate of cleaning

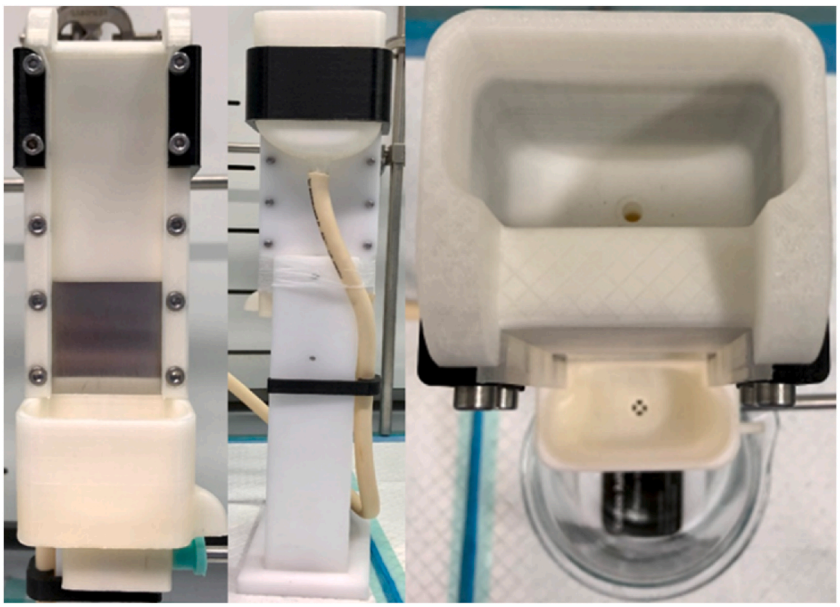

Fig. 1. Prototype of the cleaning rig, 3D-printed in PLA. (Left) Front view, (middle) back view, and (right) top view of the cleaning rig.

performance by avoiding excessive mechanical shear forces: film flow in CIP cleaning is developed on vessel walls away from the direct impingement area of the jets, and thus the mechanical action is much weaker. Furthermore, to guarantee a fully developed film flow over the coupon free from transient effects, the flow is guided on a 4" ramp for an overall aspect ratio of 3:1. Additional components required for a fully functional assembly are a feed tank through which solvent is pumped, and a drain section to collect the effluent, and pass it through the PAT probe.

The rig was 3D printed in polylactic acid (PLA) with SS316 fasteners (Fig. 1). The drain section has a concave shape, which provides a small liquid head over the probe. This reduces the risk of an air bubble being trapped in the flow path. A vortex breaker was also added at the bottom of the drain before the sensor to avoid the penetration of air pockets into the sensor lumen.

A milled acetal base was used to bolt down the rig instead of relying on laboratory stands to clamp the rig, thus reducing vibrations from the pump to the rig. 3D-printed clamps bolt over the entire assembly to improve the mechanical integrity and exert extra pressure on mating faces, which minimises the occurrence of leaks.

2.3. Coupon preparation

In this study, Olanzapine was selected as a hard-to-clean residue model. The first stage of the coupon preparation was to clean the barre stainless steel (SS) coupons with water and methanol [4,30]. Clean 2'' × SS coupons were weighed before and after being stained with either a saturated solution or a paste of Olanzapine in methanol. Coupons were prepared in triplicate, with a pipette for the saturated solution (Fig. 2), or with a spatula to smear the paste to stain the coupons (Fig. 3). All coupons were stored at 40 °C before the cleaning trials. The dirty hold time varied for each experiment, the specific amount of time that the coupons were stored at 40 °C is specified in the figure captions.

2.4. Instrumentation and data collection

The setup of the cleaning trials (Fig. 4) included a Hirschmann Rotarus smart 30 peristaltic pump, the cleaning rig, a PAT tool (Ocean Optics: STS-UV detector), DH-mini UV–Vis–NIR light source (Deuterium lamp), a T200-RT-UV-VIS transmission dip probe with a 10 mm pathlength optical chamber from Ocean Insight, and a Dell Ultrasharp WB7022 webcam.

Micrographs of the deposited olanzapine crystals were obtained using a Hitachi SU70 scanning electron microscope, at a gun voltage of 5 kV, and using a secondary electron detector at a working distance of 10 mm.

2.5. Cleaning trials

The first step to allow the cleaning trials was to collect a calibration curve for Olanzapine in methanol. The calibration curve was collected with 200 ms integration time, an average of five scans, and integrated over the main peak's wavelength range using Simpson's integration method. Application of Beer-Lambert's law on the integral of the absorption spectrum instead of the peak intensity was chosen to minimise variation in the reading, as the requirement for fast response prohibits the use of high scan averaging to combat noise.

Olanzapine solutions ranging from 1 to 50 mg L^{-1} were used to collect the calibration curve (Fig. 5) over a 250–310 nm wavelength range. Limit of Detection ($LOD = \left[3.3 \times \left(\sigma/s\right)\right]$), and Limit of Quantification ($LOQ = \left[10 \times \left(\sigma/s\right)\right]$; where s = slope of the calibration curve, σ = standard deviation of the response) were calculated from the calibration curve according to the ICH Q2(R1) guidelines [31]. Olanzapine showed a very low LOD (0.77 mg L^{-1}) and LOQ (2.35 mg L^{-1}).

Coupons would be considered clean if the stain was not visible (visually clean) [32], or when the PAT signal returned to baseline

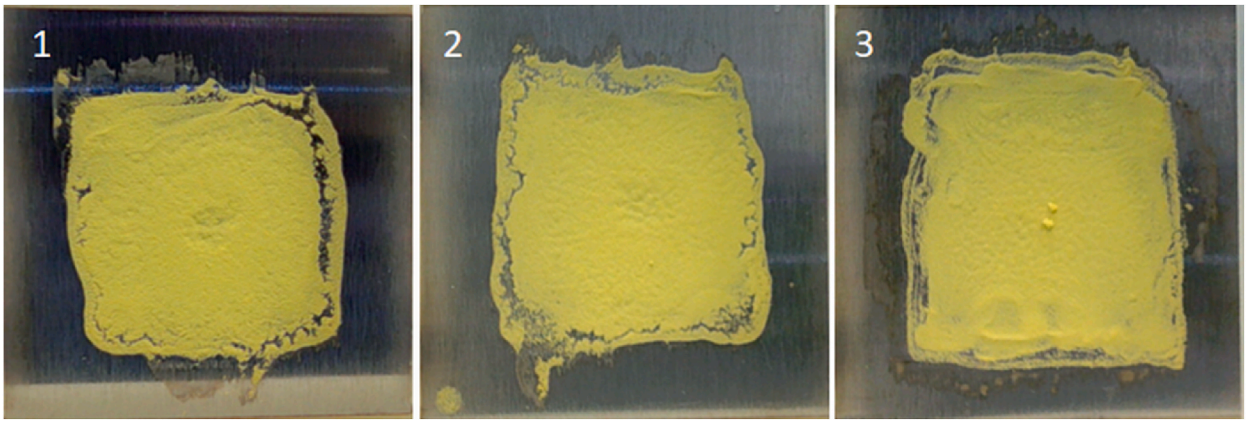

Fig. 2. Coupons #1, #2, and #3 stained with a saturated solution of Olanzapine in methanol. Coupons were stained with 300 μL. Dirty hold time was three weeks. The blue lines observed on the coupons are reflections from the laboratory lights.

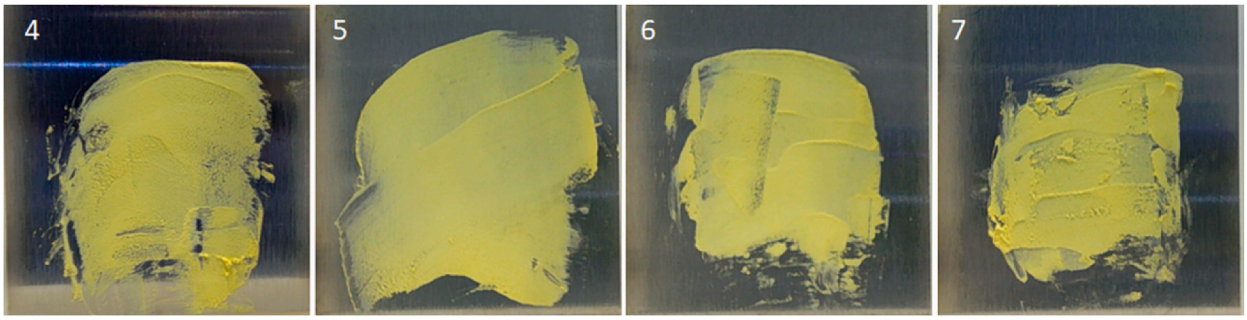

Fig. 3. Coupons #4, #5, #6, and #7 stained with a paste of Olanzapine in methanol using a spatula. Dirty hold time was 16 days. The blue lines observed on the coupons are reflections from the laboratory lights.

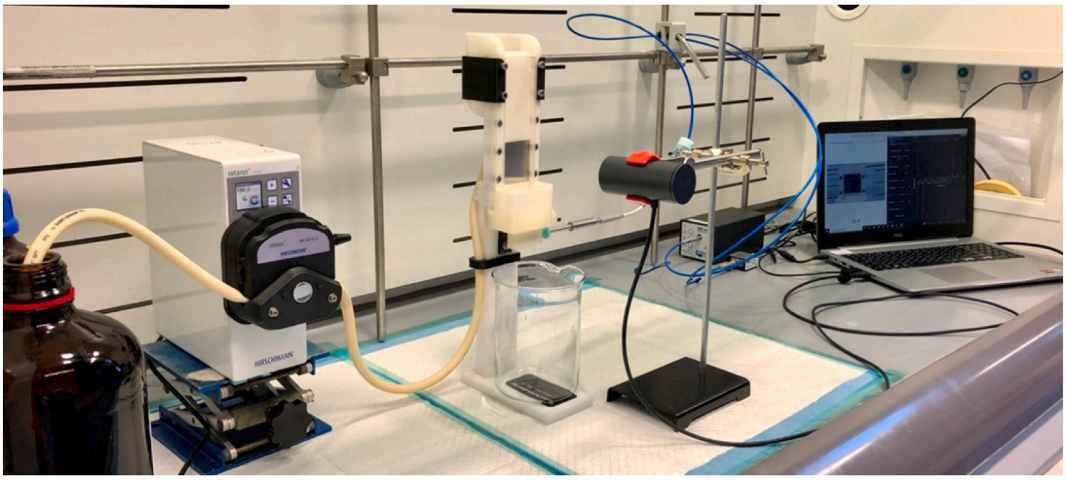

Fig. 4. Setup of the cleaning trials showing the peristaltic pump, cleaning rig, inline UV–Vis PAT tool equipped with an immersion probe, UV–Vis light source, optical camera and a computer to control the setup. The experiments were carried out inside a fume hood.

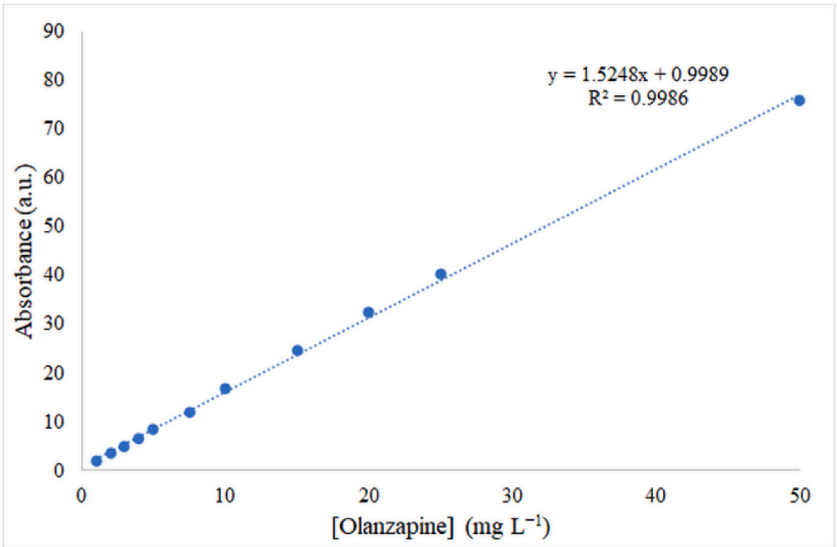

Fig. 5. Calibration curve for the Olanzapine solutions in methanol with a concentration ranging from 1 to 50 mg L^{-1}. The calibration curve was collected with the Ocean Optics STS-UV system.

levels. The endpoint of the cleaning trials would be which happened first: visually clean or return to baseline levels.

2.6. Data analysis

The concentration measured by the UV–Vis instrument was recorded, and the amount of Olanzapine cleaned was then calculated using Equation (1). All the calculations were made using an in-house written code carried out in MATLAB ver. 9.9 (The MathWorks Inc.). Raw PAT data was collected and smoothed using a 10-point moving average filter. A constant offset baseline correction was applied to correct the fluctuations going into negative values measured by the PAT tool towards the cleaning endpoint when the concentration was below detection limits. The code computes the concentration profile measured by the PAT tool and calculates the amount dissolved by the cleaning solvent according to Equation (1).

$$API\ cleaned_{mg} = \int \frac{Concentration(t)_{mg\ L^{-1}} \times Flow\ rate_{L\ min^{-1}}}{60_{s\ min^{-1}}} dt \qquad \text{Equation 1}$$

3. Results and discussions

3.1. Cleaning of olanzapine coupons prepared with a saturated solution

Coupons prepared with Olanzapine saturated solution (Fig. 2) had a dirty hold time of three weeks. The average weight of Olanzapine for the coupons prepared with 300 μL of the saturated solution was 46.60 ± 2.41 mg. The average Olanzapine residual left on the coupons after the cleaning trials was 0.37 ± 0.12 mg, with an average of 99.21 ± 0.26 % of the Olanzapine being cleaned during the trials (Table 1). The coupons were cleaned until the UV–Vis signal returned to baseline values, which happened without the coupons being visually clean (Fig. 6).

Fig. 7 exhibits the cleaning monitoring signals measured by the in-line UV–Vis. Olanzapine concentrations (D-F) and the totalized Olanzapine amounts measured by the PAT tool (A-C) are shown. The first trial (Fig. 7A-D) shows a typical cleaning profile: there is an initial concentration spike corresponding to the initial removal of most of the loosely bound soil and a decaying tail that corresponds to the dissolution of the remaining bound layer.

The totalized removed soil (Fig. 7A) shows that the majority of the soil is indeed removed in the first 10 s. The second and third trials (Fig. 7B-E and 7C–7F) show a more complex behaviour, with a primary peak and a secondary peak observed, causing two plateaus in the totalized Olanzapine detected (Fig. 7B-C). This behaviour is not characteristic of surface cleaning phenomena based on soil dissolution. Olanzapine cleaned from Coupons #2 and #3 was removed in sizeable flakes that broke off the surface, as opposed to the more dispersive removal observed in Coupon #1. These solid flakes are deposited in the bottom of the drain section upstream of the UV–Vis probe, disintegrating and dissolving there due to the higher flow velocity at the throat, thus giving an artificial second peak. However, the totalized amount of Olanzapine removed did account for this secondary dissolution phenomenon, and therefore increased the recovery, nonetheless. Table 2 summarises the cleaning results.

The low recovery calculated with Equation (1) can be explained by the fast washout of the Olanzapine on the coupons prepared with the saturated solution. The Olanzapine applied to the coupons was almost completely washed out in a few milliseconds (Video 1, https://youtu.be/C6sX4Mot1Rs). These data show that the UV–Vis PAT technique used for monitoring the cleaning process can only monitor the dissolved API, and therefore mechanically entrained API that was not dissolved passed through the sensor without being detected, hence the low recovery calculated.

3.1.1. Cleaning of olanzapine coupons prepared using a paste

The dirty hold time for the coupons prepared with Olanzapine paste (Fig. 3) was 16 days. The average Olanzapine weight for the coupons prepared with the paste was 30.48 ± 2.68 mg, and an average residual of 3.10 ± 1.74 mg was left on the coupons after the cleaning trials. An average of 89.78 ± 5.54 % of the Olanzapine was cleaned from the coupons during the cleaning trials (Table 3). The coupons were not visually cleaned (Fig. 8) even after 2.5/3 min on stream, after which the experiments had to be stopped due to the solvent being consumed totally. Experiments were limited to the use of a 2.5 L bottle of methanol per coupon.

After the cleaning trials, the amount of Olanzapine cleaned was calculated (Equation (1), Table 4) from the concentration measurements recorded from the UV–Vis PAT tool.

While the washout was the main cleaning mechanism observed for the coupons prepared from the saturated solution of Olanzapine, dissolution was prevalent for the coupons prepared from the paste. This can be observed in Fig. 9. The amount of Olanzapine cleaned

Table 1
Olanzapine saturated solution (300 μL) was applied to the coupons with a pipette. All the coupons were dried at 40 °C for three weeks. Olanzapine concentration ($mg.L^{-1}$) was measured online using the Ocean Optics STS-UV system.

Coupon #	Coupon (g)	Coupon + Olanzapine (g)	Olanzapine (mg)	Coupon after cleaning (g)	Total amount cleaned (mg)	Residual (mg)	% Cleaned
1	20.0800	20.1290	49.00	20.0805	48.50	0.5	98.98
2	20.1288	20.0815	47.50	20.0815	47.30	0.20	99.58
3	20.0469	20.0902	43.30	20.0473	42.90	0.40	99.08

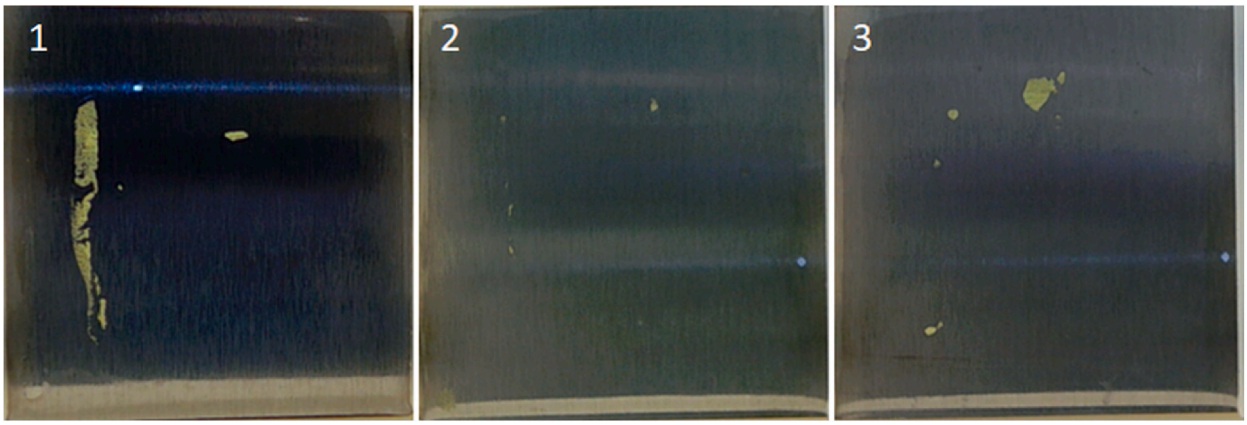

Fig. 6. Coupons #1, #2, and #3 after being cleaned with methanol at 0.8 L min^{-1} flow rate. The blue lines observed on the coupons are reflections from the laboratory lights.

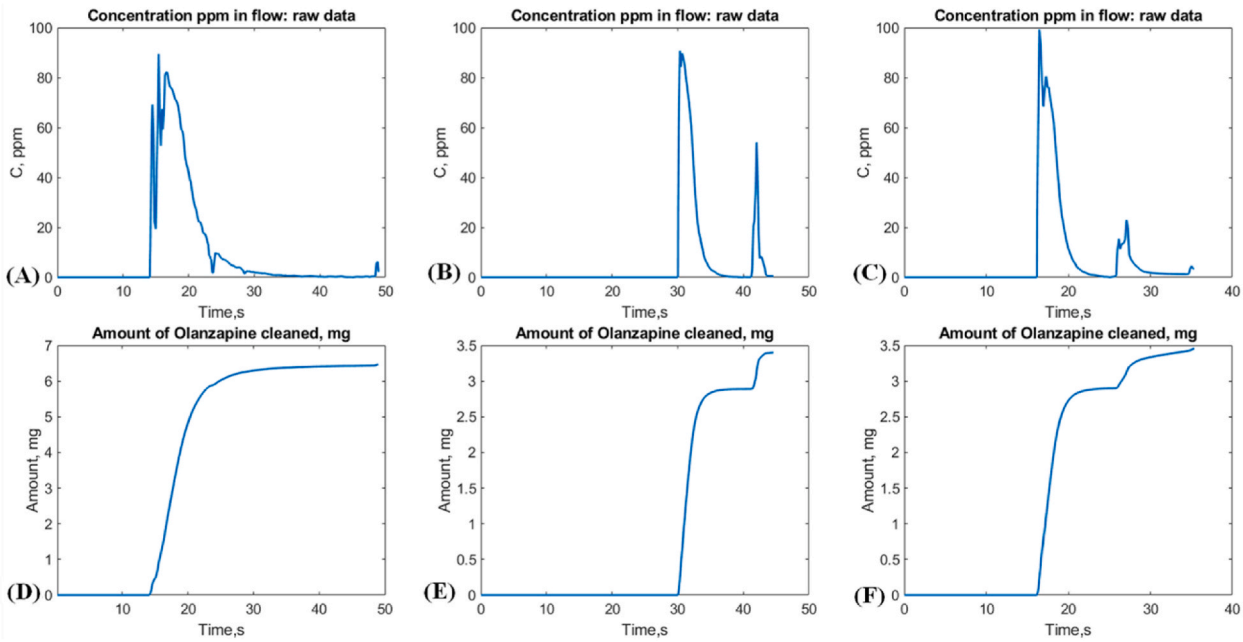

Fig. 7. The top row shows the graphs of time *vs.* concentration of Olanzapine cleaned out for (A) Coupon #1, (B) Coupon #2, and (C) Coupon #3. The bottom row shows the graphs of time *vs. the* amount of Olanzapine cleaned (D) Coupon #1, (E) Coupon #2, and (F) Coupon #3.

Table 2
Olanzapine concentration ($mg.L^{-1}$) was measured online using the Ocean Optics STS-UV system. The stain area was different for each coupon.

Coupon #	Amount of Olanzapine cleaned (mg)	Time to clean (s)	% Recovery	Coupon area stained (cm^2)
1	6.47	24.77	13.2	12.3325
2	3.40	13.3	7.16	12.5694
3	3.44	18.37	7.98	13.4074

increased with time (Fig. 9A–D), the first spike observed in Fig. 9 (E-H) was due to some small shear off, with a constant concentration being washed out for the rest of the cleaning time. Even though it looks like Coupon #6 did not follow this pattern, the presence of two other peaks (Fig. 9G) was artificially created by the change in the bottle of methanol being used for the cleaning process. The methanol flow was momentarily interrupted during the change, meaning that there was a break of the meniscus in the sensor, artificially creating the peaks observed in Fig. 9G.

Most of the Olanzapine paste coupons had a good, calculated recovery (>79 %), except Coupon #7. The poor recovery in the last

Table 3
Olanzapine paste was applied with the help of a spatula on the coupons. All the coupons were dried at 40 °C for 16 days. Olanzapine concentration (mg.L^{-1}) was measured online using the Ocean Optics STS-UV system.

Coupon #	Coupon (g)	Coupon + Olanzapine (g)	Olanzapine (mg)	Coupon after cleaning (g)	Total amount cleaned (mg)	Residual (mg)	% Cleaned
4	20.0534	20.0842	30.80	20.0585	25.70	5.1	83.44
5	19.7977	19.8240	26.30	19.7995	24.50	1.80	93.16
6	20.0746	20.1056	31.00	20.0791	26.50	4.5	85.48
7	19.8884	19.9222	33.80	19.8894	32.80	1.0	97.04

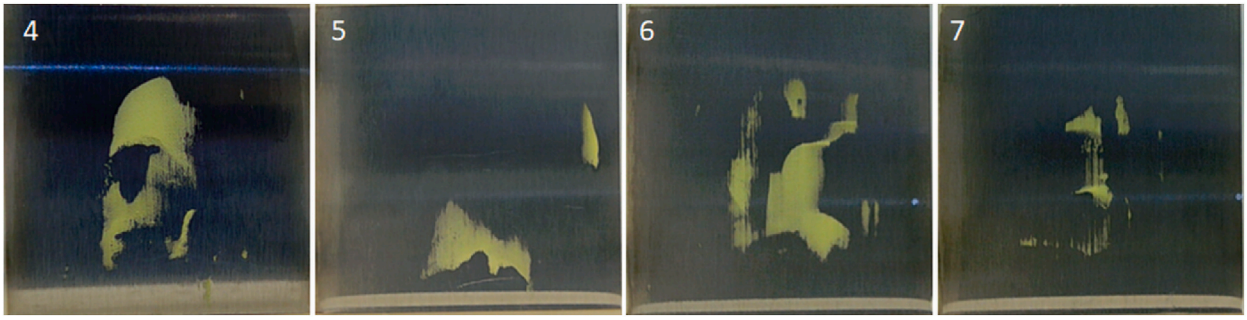

Fig. 8. Coupons #4, #5, #6, and #7 after being cleaned with methanol at 0.8 L min^{-1} flow rate. The blue lines observed on the coupons are reflections from the laboratory lights.

Table 4
Olanzapine concentration (mg.L^{-1}) was measured online using the Ocean Optics STS-UV system. The stain area was different for each coupon.

Coupon #	Amount of Olanzapine cleaned (mg)	Time to clean (s)	% Recovery	Coupon area stained (cm^2)
4	24.54	133.47	79.68	12.9776
5	24.53	142.6	82.28	15.7743
6	26.16	175.8	84.28	11.5005
7	16.74	147.27	49.59	11.0647

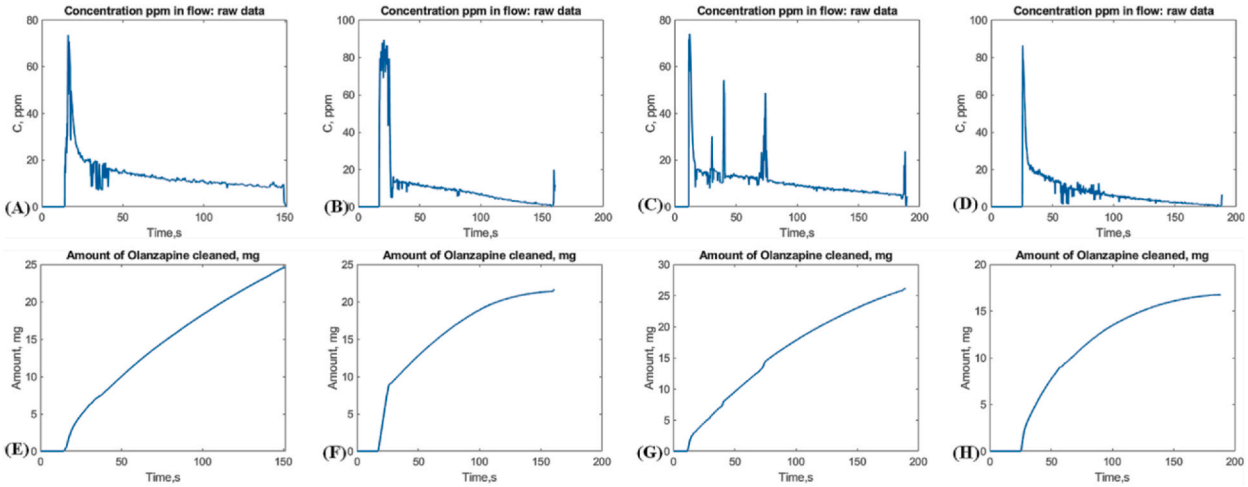

Fig. 9. The top row shows the graphs of time *vs.* concentration of Olanzapine cleaned out (A) Coupon #4, (B) Coupon #5, (C) Coupon #6, and (D) Coupon #7. The bottom row shows the graphs of time *vs.* amount of Olanzapine cleaned for (E) Coupon #4, (F) Coupon #5, (G) Coupon #6, and (H) Coupon #7. Multiple spikes in Coupon #6 occurred during the change of the methanol bottle.

coupon (49 %) was associated with the significant shear-off at the beginning of the cleaning (Video 2, https://youtu.be/lvk37NF_7OQ). The mechanically displaced soil (shear off) was not detected by PAT, hence the low calculated recovery observed for Coupon #7. The slightly reduced recovery calculated from the concentration measured with the PAT tool for Coupons #4 to 6 could

also be explained by shearing off of Olanzapine material during the cleaning trial (Video 3, https://youtu.be/lrOw8w1_gWs). Only the API that undergoes dissolution could be measured with the Ocean Optics UV–Vis system, thus, the shear off influenced the calculated recovery. The shear-off was minimal for the coupons prepared with a paste, with dissolution being the main mechanism responsible for their cleaning.

While the scope of this study is the demonstration of the usefulness experimental rig equipped with UV–Vis as a PAT tool to develop cleaning methodologies and study the cleaning mechanisms, the obtained results show some limitations of the use of UV–Vis as a unique PAT tool. If the dissolved amount of olanzapine is below the detection limit, UV–Vis is not sufficient to detect the residues. Thus, combining UV–Vis with another optical PAT tool is necessary to visually ensure the cleanness of the coupons. Of note, pharmaceutical industries are relying on visual inspection to validate the cleaning process.

Cleaning of the Olanzapine coupons prepared with the paste was less efficient than those prepared from the saturated solution, even if the dirty hold time was smaller. This could be explained by the difference in Olanzapine crystal sizes between the coupons prepared with a saturated solution and a paste (Fig. 10). The recrystallization occurring during the natural drying of the saturated solution produced a crystal size distribution that was larger than the original crystal size distribution of the olanzapine dispersed in methanol as a paste. Smaller particles are more difficult to remove [33], thus, it was natural that the coupons prepared with a paste were harder to clean. The difference in crystal sizes was not related to the formation of different Olanzapine polymorphs [34,35]. In addition to experiencing a lower rotational torque under the flow, smaller crystals also interact more closely with the surface crevices, which makes their displacement by fluid flow more challenging.

There are two mechanisms governing CIP cleaning: dissolution and mechanical entrainment. Our study shows that only dissolution could be efficiently tracked by the UV–Vis PAT. The origin of the Olanzapine stain affects its mechanical properties, and therefore the dominating cleaning mechanism in the cleaning process is dependent on the crystallization and agglomeration conditions.

To use the bench scale results to optimize CIP cleaning parameters accurately, knowledge of the soil conditions inside process equipment is crucial to selecting the proper coupon staining method. Practically, different areas of the processing equipment will have different soil conditions, and therefore real equipment will show an intermediate behaviour between both extremes. In a typical crystallization vessel, the metal surface in contact with the top of the liquid level is continuously swept by oscillating liquid levels that create a thin film, and the occasional splashes of saturated liquor. Drying of these layers is likely to produce stains of properties comparable to those prepared by saturated solution. The submerged parts of the vessel, especially at the bottom, will typically be stained with a cake-like deposit of crystals carried by the solvent, and eventually dry into stains comparable with the dried paste prepared. Therefore, cleaning of the vessel will be governed by a mutual contribution of both mechanisms.

The implication of these findings in terms of CIP design for an Olanzapine processing facility highlights the resilience of Olanzapine stains to removal by mechanical dislodgement during the initial gross rinse. Thus, it is necessary to use high shear and potentially impact jets during the initial rinse to successfully remove the majority of Olanzapine, before running the subsequent cleaning passes that eventually dissolve the strongly bound final layer. The use of in-line PAT in this application would be targeted towards the detection and verification of the cleaning endpoint rather than the quantification of the total amount removed.

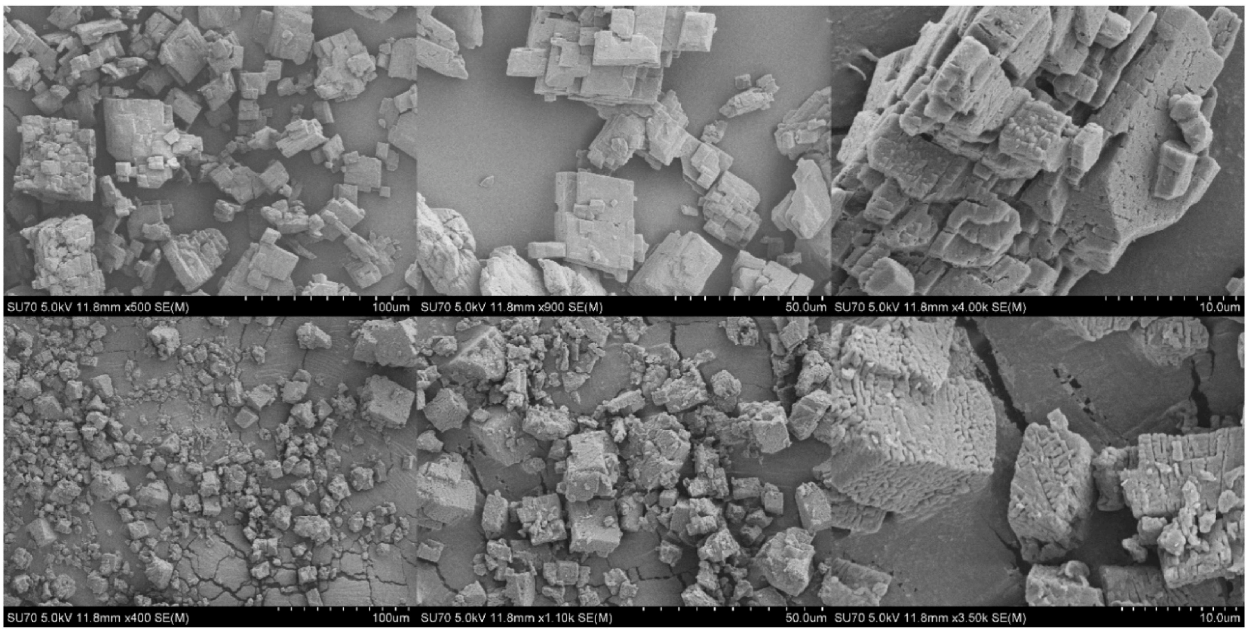

Fig. 10. Scanning electron micrographs of the olanzapine (top) prepared from saturated solution, (bottom) prepared with Olanzapine paste, before being cleaned.

4. Conclusions

Throughout this study, the application of the in-line UV–Vis PAT tool in the real-time monitoring of cleaning-in-place was comprehensively investigated. PAT technology was assessed for the in-situ monitoring of cleaning progress. The use of in-line UV–Vis as a PAT tool is useful to monitor the cleaning profile and to verify the cleaning performance but cannot be used to quantify the total amount of soil washed out. Thus, combining UV–Vis with another PAT tool like an optical PAT is necessary to ensure the cleanness of the surface. Its use in recovery studies during cleaning validation studies should be accompanied by another PAT technique capable of quantifying dispersed but non-dissolved API. Future designs should include the integration of multiple PAT tools for more reliable measurements.

Olanzapine was shown to be a difficult material to clean, and its cleaning profile was tremendously affected by the properties of the stain. This shows that the development of bench-scale studies for CIP process optimization must therefore consider the different soil qualities on process equipment and attempt to replicate them as closely as possible. The obtained data showed that methanol is not the best cleaning agent for Olanzapine. Long times and large volumes of methanol are required for an efficient cleaning of Olanzapine. Further cleaning trials should assess the use of other solvents or optimized solvent blends that show a higher olanzapine solubility.

The cleaning trials showed that the cleaning mechanism of olanzapine is governed by lift-off and dissolution. Thus, adhesion properties and interactions with the cleaning agent should be considered when investigating other APIs with similar properties as olanzapine. These findings pave the way to develop methodologies that can be applied to groups of APIs with similar physical and chemical properties.

The film flow rig developed in this work is ideal to optimize the cleaning process by assessing other cleaning agents, as long as the rig is printed in a more chemical-resistant material. The next steps are to manufacture the film flow rig with polyether ether ketone (PEEK), which should allow the use of different solvents to select the best one to be used.

Data availability statement

The raw data required to produce this paper will be provided if requested.

CRediT authorship contribution statement

Marina Steiner-Browne: Writing – review & editing, Writing – original draft, Methodology, Investigation, Formal analysis, Data curation, Conceptualization. **Nicolas Abdel Karim Aramouni:** Writing – review & editing, Writing – original draft, Methodology, Investigation, Formal analysis, Data curation, Conceptualization. **Rabah Mouras:** Writing – review & editing, Writing – original draft, Supervision, Project administration, Investigation, Funding acquisition, Conceptualization.

Declaration of competing interest

The authors declare that they have no known competing financial interests or personal relationships that could have appeared to influence the work reported in this paper.

Acknowledgments

The authors thank Orest Shardt and Mohsen Hassanzadeh Moghimi for their advice and contribution to the design of the film flow rig used in the current study. We also thank Eli Lilly for the Olanzapine in-kind contribution.

The research conducted in this publication was funded by Enterprise Ireland through the PMTC core cleaning project (TC-2018-0026) and the Innovation partnership program (IP-2020-0957).

References

[1] J. Wiss, J.L. Schmuck, Cleaning validation using thermogravimetry, J. Therm. Anal. Calorim. 104 (1) (2011) 315–321.
[2] G. Mordue, Cleaning verification & validation of multipurpose API plants: 9 rules to follor, in: https://www.bioprocessonline.com/doc/cleaning-verification-validation-of-multipurpose-api-plants-rules-to-follow-0001, 2021.
[3] E.V. Sargent, et al., The regulatory framework for preventing cross-contamination of pharmaceutical products: history and considerations for the future, Regul. Toxicol. Pharmacol. 79 (2016) S3–S10.
[4] I.A.H. Ahmad, et al., Cleaning verification: exploring the effect of the cleanliness of stainless steel surface on sample recovery, J. Pharmaceut. Biomed. Anal. 134 (2017) 108–115.
[5] H.M. Sheng, et al., Development of an automated and High throughput UHPLC/MS based workflow for cleaning verification of potent compounds in the pharmaceutical manufacturing environment, J. Pharmaceut. Biomed. Anal. (2020) 188.
[6] S.L. Prabu, T.N.K. Suriya Prakash, R. Thirumurugan, Chapter 5 - cleaning validation and its regulatory aspects in the pharmaceutical industry, in: R. Kohli, K. L. Mittal (Eds.), Developments in Surface Contamination and Cleaning, William Andrew Publishing, Oxford, 2015, pp. 129–186.
[7] I.I. Valvis, W.L. Champion, Cleaning and decontamination of potent compounds in the pharmaceutical industry, Org. Process Res. Dev. 3 (1) (1999) 44–52.
[8] P.I.C.-o. Scheme, Guideline on Setting Health Based Exposure Limits for Use in Risk Identification in the Manufacture of Different Medicinal Products in Shared Facilities, 2018.
[9] D.-G.f.H.a.F.S. European Union, Annex 15: qualification and validation, in: EU Guidelines for Good Manufacturing Practice for Medicinal Products for Humand and Veterinary Use, 2015.
[10] FDA, Guidance for Industry, PAT - A Framework for Innovative Pharmaceutical Development, Manufacturing, and Quality Assurance, 2004.

[11] M.A. Druy, Applications for mid-IR spectroscopy in the pharmaceutical process environment - mid-IR continues to prove its usefulness as a process analytical technology, Spectroscopy 19 (2) (2004) 60–63.
[12] A. Sarwar, et al., Investigation of an alternative approach for real-time cleaning verification in the pharmaceutical industry, Analyst 145 (22) (2020) 7429–7436.
[13] L. Alvarez-Jubete, et al., Feasibility of near infrared chemical imaging for pharmaceutical cleaning verification, J. Near Infrared Spectrosc. 21 (3) (2013) 173–182.
[14] H.M. Sheng, et al., Combined chromatographic and spectrometric approaches for cleaning verification of small-molecule pharmaceutical compounds in the manufacturing environment, LC-GC N. Am. 39 (4) (2021) 187.
[15] N. Rathore, W. Qi, W.C. Ji, Cleaning characterization of protein drug products using UV-vis spectroscopy, Biotechnol. Prog. 24 (3) (2008) 684–690.
[16] M. Spoerk, et al., Novel cleaning-in-place strategies for pharmaceutical hot melt extrusion, Pharmaceutics 12 (6) (2020).
[17] K. Chullipalliyalil, L. Lewis, M.A.P. McAuliffe, Deep UV laser-induced fluorescence for pharmaceutical cleaning validation, Anal. Chem. 92 (1) (2020) 1447–1454.
[18] V. Behrendt, A. Blättermann, A. Brandenburg, A fiber-optical fluorescence sensor for in-line determination of cleanliness during CIP processes, Food Bioprod. Process. 137 (2023) 56–63.
[19] N.K. Mehta, et al., Development of an in situ spectroscopic method for cleaning validation using mid-IR fiber-optics, Biopharm-the Applied Technologies of Biopharmaceutical Development 15 (5) (2002) 36.
[20] E.L. Simmonds, W.J. Lough, M.R. Gray, Evaluation of LC-MS for the analysis of cleaning verification samples, J. Pharmaceut. Biomed. Anal. 40 (3) (2006) 631–638.
[21] J. Escrig, et al., Clean-in-place monitoring of different food fouling materials using ultrasonic measurements, Food Control 104 (2019) 358–366.
[22] F. Destro, M. Barolo, A review on the modernization of pharmaceutical development and manufacturing - trends, perspectives, and the role of mathematical modelling, Int. J. Pharm. 620 (2022) 121715.
[23] A. Aina, et al., Exploring the advantages of PAT for pharmaceutical cleaning in Ireland, European Pharmaceutical Review 21 (2) (2016) 44–46.
[24] C.B. Lyndgaard, et al., Moving from recipe-driven to measurement-based cleaning procedures: monitoring the Cleaning-In-Place process of whey filtration units by ultraviolet spectroscopy and chemometrics, J. Food Eng. 126 (2014) 82–88.
[25] H. Kohler, et al., How to assess cleaning? Evaluating the cleaning performance of moving impinging jets, Food Bioprod. Process. 93 (2015) 327–332.
[26] E. Rivera, P. Lopolito, Evaluating surface cleanliness using a risk-based approach, Biopharm Int. 30 (11) (2017) 36–+.
[27] E. Manning, et al., Application of lean six sigma to optimize a legacy cleaning process, Pharmaceut. Eng. 34 (2014) 50–59.
[28] I. Palabiyik, et al., Optimization of temperature for effective cleaning with a novel cleaning rig: influence of soil and surface types, Food Bioprod. Process. 136 (2022) 36–46.
[29] L.D. Silva, et al., Optimization of clean-in-place (CIP) procedure of pipelines contaminated with Bacillus cereus by applying pulsed flow, Food Control (2023) 147.
[30] I.A.H. Ahmad, A. Blasko, Failure of cleaning verification in pharmaceutical industry due to uncleanliness of stainless steel surface, Jove-Journal of Visualized Experiments 126 (2017).
[31] P. Borman, D. Elder, Q2(R1) validation of analytical procedures, in: ICH Quality Guidelines, 2017, pp. 127–166.
[32] R.J. Forsyth, V. Van Nostrand, G.P. Martin, Visible-residue limit for cleaning validation and its potential application in a pharmaceutical research facility, Pharmaceut. Technol. 28 (2004) 58–72.
[33] G.Z. Li, et al., A review of factors affecting the efficiency of clean-in-place procedures in closed processing systems, Energy 178 (2019) 57–71.
[34] C.G. Testa, et al., Challenging identification of polymorphic mixture: polymorphs I, II and III in olanzapine raw materials, Int. J. Pharm. 556 (2019) 125–135.
[35] S.M. Reutzel-Edens, R.M. Bhardwaj, Crystal forms in pharmaceutical applications: olanzapine, a gift to crystal chemistry that keeps on giving, Iucrj 7 (2020) 955–964.